Materials Chemistry and Physics 250 (2020) 123134

Contents lists available at ScienceDirect

Materials Chemistry and Physics

journal homepage: www.elsevier.com/locate/matchemphys

A novel high-Q and low-temperature sintering $Li_2Mg_3Ti_{1-x}(Al_{1/2}Nb_{1/2})_xO_6$-4wt%LiF microwave dielectric ceramics

Ping Zhang *, Gaowei Zhen, Miaomiao Yang

School of Electrical and Information Engineering and Key Laboratory of Advanced Ceramics and Machining Technology of Ministry of Education, Tianjin University, Tianjin, 300072, China

HIGHLIGHTS

- A novel high-Q $Li_2Mg_3Ti_{1-x}(Al_{1/2}Nb_{1/2})_xO_6$-4wt%LiF($0.02 \leq x \leq 0.08$) ceramics were prepared by solid stated reaction.
- The $Q \times f$ value of ceramics was increased by the substitution of $(Al_{1/2}Nb_{1/2})^{4+}$.
- The $Li_2Mg_3Ti_{0.96}(Al_{1/2}Nb_{1/2})_{0.04}O_6$-4wt%LiF ceramics sintered at 900 °C exhibited excellent microwave dielectric properties.

ARTICLE INFO

Keywords:
$Li_2Mg_3TiO_6$-4wt%LiF ceramics
Microwave dielectric properties
Sintering characteristics
Composite ions
$(Al_{1/2}Nb_{1/2})^{4+}$

ABSTRACT

A novel system $Li_2Mg_3Ti_{1-x}(Al_{1/2}Nb_{1/2})_xO_6$-4wt%LiF($0.02 \leq x \leq 0.08$) ceramics were synthesized by the solid stated reaction method to improve the microwave dielectric properties of the ceramics. The phase composition, sintering characteristics and microwave dielectric properties of $Li_2Mg_3Ti_{1-x}(Al_{1/2}Nb_{1/2})_xO_6$-4wt%LiF($0.02 \leq x \leq 0.08$) ceramics were then explored. The results demonstrated that at the optimal sintering temperature(900 °C), with the $(Al_{1/2}Nb_{1/2})^{4+}$ ions increased, the ε_r value decreased and the absolute value of τ_f augmented. Moreover, the $Q \times f$ value of ceramics was in accord with the relative density, which enlarged at first until the doping content reached the solid solubility limit (0.04 mol) of the ceramics. In total, the $Li_2Mg_3Ti_{1-0.96}(Al_{1/2}Nb_{1/2})_{0.04}O_6$-4wt%LiF ceramics sintered at 900 °C for 6 h showed the best microwave dielectric properties of ε_r~15.54, $Q \times f$~154,000 GHz and τ_f~-38.3 ppm/°C.

1. Introduction

As the quickly changing and enormous progress of the information technology, aerospace and military industries, the demand for communication microwave components and the requirements for their quality are increasing. Therefore, it is of considerable significance to search for microwave dielectric ceramics that can not only be prepared at low temperature but also have excellent performance for the progress of science and technology and the development of passive devices [1–3]. The organic electronic functional materials and multiferroic materials both have been researched extensively [4–7]. Microwave dielectric ceramics, as a kind of functional electronic ceramics developed recently, should be satisfied with the following dielectric characteristics: high quality factor ($Q \times f$) value, an appropriate dielectric constant (ε_r) and temperature coefficient of resonant frequency (τ_f) near to zero [8,9].

The Li-based oxide ceramics such as Li_2MgTiO_4, $Li_2MgTi_3O_8$ and $Li_2Mg_3BO_6$ (B = Ti, Sn, Zr) have been proved to own excellent microwave dielectric properties [10–18]. Moreover, the sintering temperature should be lower for LTCC applications. Adding sintering additives is the preferred method to reduce the sintering temperature. Sintering additives are mainly divided into oxides (such as B_2O_3, CuO), composite glass (such as ZBS, LBS), compounds (such as LiF) and composite additives (such as LiF–V_2O_5–CuO) [19]. Zhifen Fu et al. studied to add different sintering additives LC (2 wt%LiF + 2 wt%CuO) into $Li_2Mg_3TiO_6$ ceramics to reduce the sintering temperature. However, the τ_f still shows a large negative value and $Q \times f$ value is low in this method [11]. Based on this, this team synthesized $0.9Li_2Mg_3TiO_6$-$0.1SrTiO_3$-4wt%LiF to improve τ_f, but the $Q \times f$ value was still a question [12]. Nowadays, $Li_2Mg_3TiO_6$-4wt%LiF has attracted a lot of attention for its low-temperature sintering characteristic and good τ_f value, but the $Q \times f$ value is low as well [20]. Recently, the researchers found that high $Q \times f$ value could be achieved by replacing Ti^{4+} with composite ionic [21–26]. Zhe Xiong et al. have reported that $(Al_{1/2}Nb_{1/2})^{4+}$ had a positive impact on dielectric characteristics of $Ba_{3.75}Nd_{9.5}Ti_{18}O_{54}$ ceramics [21].

* Corresponding author.
E-mail address: zhangping@tju.edu.cn (P. Zhang).

https://doi.org/10.1016/j.matchemphys.2020.123134
Received 21 February 2020; Received in revised form 24 April 2020; Accepted 27 April 2020
Available online 7 May 2020

$CaTi_{1-x}(Al_{0.5}Nb_{0.5})_xO_3$ ceramics studied by G.H. Chen et al. showed a ε_r~52.6, Q × *f*~22,914 GHz and τ_f~6.4 ppm/°C [22]. Besides, a low-temperature sintering $Li_2Ti_{1-x}(Al_{0.5}Nb_{0.5})_xO_3$ ceramics researched by T.W Zhang et al. showed excellent ε_r ~21.2, Q × *f* ~181,800 GHz and τ_f~12.8 ppm/°C [23]. Therefore, investigating the effects of $(Al_{1/2}Nb_{1/2})^{4+}$ on $Li_2Mg_3TiO_6$-4wt%LiF ceramics to improve the Q × *f* value has become essential things that should be addressed urgently.

Here in this work, sintering by conventional solid stated reaction method, the microwave dielectric properties of $Li_2Mg_3TiO_6$-4wt%LiF ceramics has been improved by replacing the B-site Ti^{4+} ions of the ceramics with composite ions $(Al_{1/2}Nb_{1/2})^{4+}$. Then, microstructure, the phase composition and sintering characteristics of the $Li_2Mg_3Ti_{1-x}(Al_{1/2}Nb_{1/2})_xO_6$-4wt%LiF (LMTAN for short) ($0.02 \le x \le 0.08$) ceramics sample was observed and studied. Besides, we deeply analyzed the variations of microwave dielectric properties, including dielectric(ε_r), quality factors(Q × *f*) and temperature coefficient of resonant frequency (τ_f). Finally, we primarily investigated the effect of $(Al_{1/2}Nb_{1/2})^{4+}$ ions doped to the improvement of the Q × *f* value, which could be more suitable for modern information devices.

2. Experimental procedure

Firstly, high purity (≥99%) Li_2CO_3, TiO_2, MgO, Nb_2O_5, Al_2O_3, and LiF powders were used as starting materials and mixed in terms of the chemical formula $Li_2Mg_3Ti_{1-x}(Al_{1/2}Nb_{1/2})_xO_6$ (x = 0.02, 0.04, 0.06, 0.08). Then, the materials were added together with deionized water for ball grinding by zirconium balls for 8 h. The materials after dried and screened were pre-fired at 1000 °C for 4 h. After that, the second batch was carried out, which weighed 4 wt% LiF according to the quality of the pre-fired powders and ground with the after-pre-fired powders for 8 h. Then, the processed materials granulated after mixed with 5 wt%-7wt% paraffin, afterward, at the 200 Mpa pressure, the powders were compressed into a Φ10mm cylinder with the height of 5 mm. Finally, the ceramic body was completed after sintered at 850–950 °C for 6 h and then cooled down to room temperature in the furnace.

The X-ray diffraction (Rigaku D/max 2550 PC, Tokyo, Japan) was used to measure the crystalline structures of the LTMAN ceramics over 30–100°. The scanning electron microscopy (ZEISS MERLIN Compact, Germany) was used to observe the microstructure of the ceramics. And a network analyzer (N5234A, Agilent Co, America) was used to study the microwave dielectric properties of all samples in the frequency range of 7–14 GHz [27]. Among which the τ_f was measured from 25 °C to 85 °C could be calculated according to the following equation:

$$\tau_f = \frac{f_{T_2} - f_{T_1}}{f_{T_2}(T_2 - T_1)} \times 10^6 (ppm/^\circ C) \quad (1)$$

In which f_{T2} is the resonant frequency at 85 °C and f_{T1} is that at 25 °C. The relative density could be calculated by the following equation:

$$\rho_{relative} = \frac{\rho_{bulk}}{\rho_{theory}} \times 100\% \quad (2)$$

where the ρ_{bulk} and ρ_{theory} are bulk density and theoretical density, respectively. The bulk density is usually researched by the Archimedes method and the ρ_{theory} can be calculated as follows:

$$\rho_{theory} = \frac{ZA}{V_c N_A} \quad (3)$$

In which *A* and *Z* are the weight of the atom and the atom number in a unit cell. V_c and N_A are the unit cell's volume and Avogadro number [28].

3. Results and discussion

Fig. 1 displays the XRD pattern of LMTAN sintered at 900 °C for 6 h, the insert picture is the magnified patterns of specific peaks. It can be observed that when $0.02 \le x \le 0.04$, the samples show the characteristics of the rock-salt structure, in which all the diffraction peaks exhibit to the $Li_2Mg_3SnO_6$-like (PDF#39–0932) standard card, all the diffraction peaks shift to higher angle compared with standard card because the radius of Ti^{4+} and Sn^{4+} are different, and no other diffraction peaks could be found. However, when $x > 0.04$, the second phase can be detected apart from the main crystal phase $Li_2Mg_3TiO_6$, which is identified compared to the $MgAlO_4$ phase by Jade software. Furthermore, it can be concluded from the XRD picture that when $x \le 0.04$, all of the $(Al_{1/2}\ Nb_{1/2})^{4+}$ replaced the Ti^{4+} and occupied the position of Ti^{4+} ions in the lattice and formed a solid solution, because of approximate radius size between the $(Al_{1/2}\ Nb_{1/2})^{4+}$ (R = 0.588 Å, CN = 6) and the Ti^{4+} (R = 0.605 Å, CN = 6). For this reason, the diffraction peaks shift to higher angle when $0.02 \le x \le 0.04$ in the insert picture, when $x > 0.04$, the diffraction peaks stop shift because the second phase has been formed. So, the limit of the solid solution is 0.04 mol.

Fig. 2 exhibits the microstructure of LMTAN sintered at 900 °C for 6 h. In summary, all samples are presented to be densified. It is observed that the grain size increases significantly when $0.02 \le x \le 0.04$, because of the $(Al_{1/2}\ Nb_{1/2})^{4+}$ composite ions are dissolved in $Li_2Mg_3TiO_6$-4wt% LiF ceramic crystal, which reduces the free energy of the ceramic and promotes the sintering process [29]. However, the average grain size decreases and the grain shape varies as x increasing. It can be owing to the too much $(Al_{1/2}Nb_{1/2})^{4+}$ composite ions were added to form the second phase and the appearance of oxygen vacancy makes the grain grow abnormally, which thus inhibits the growth of a part of grains. Meanwhile, when x = 0.08, the samples are in uniform size and there are round dots grain formation at the grain boundary, due to the dot precipitation at the grain boundary of the aluminum element in the substitution process of $(Al_{1/2}Nb_{1/2})^{4+}$ ions, which can be found in the study of Li et al. [30]. The driving force of ceramic sintering is grain boundary energy, and impurities at grain boundary make grain boundary energy decrease, which reduces the ion diffusion rate during the sintering process and inhibits the growth of grain. Consequently, it has a negative impact on microwave dielectric properties of the ceramics.

To demonstrate the relationship between relative density and sintering temperature, we plot the relative density of LMTAN ceramics versus sintering temperatures, as is shown in Fig. 3, which has illustrated the relative density of LMTAN ceramics augment at first and then decrease with the rising of sintering temperature. The relative density of all samples reaches the best value at 900 °C, indicating that the optimum sintering temperature of samples is 900 °C. At the optimal sintering temperature, with the enhancement of the substitution amount of $(Al_{1/}$

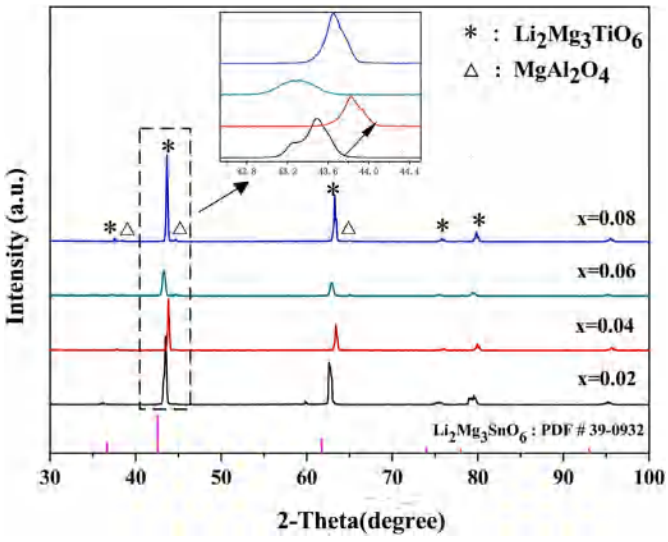

Fig. 1. The XRD patterns of $Li_2Mg_3Ti_{1-x}(Al_{1/2}Nb_{1/2})_xO_6$-4wt%LiF ceramics sintered at 900 °C for 6 h.

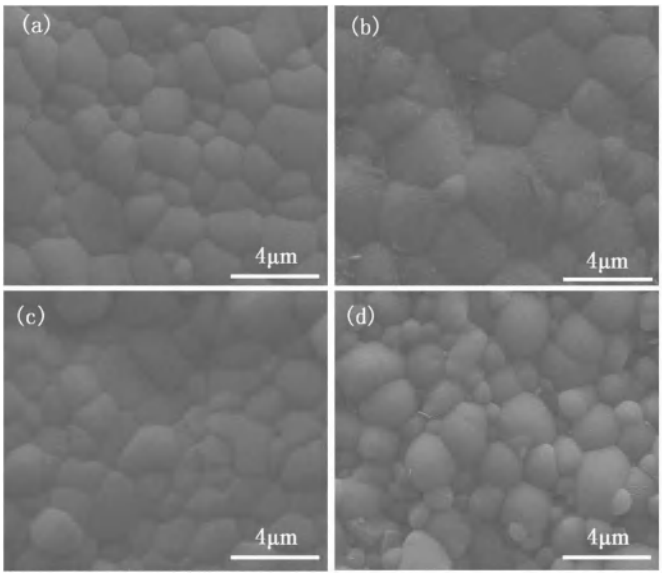

Fig. 2. The SEM photographs of $Li_2Mg_3Ti_{1-x}(Al_{1/2}Nb_{1/2})_xO_6$-4wt%LiF ceramics doped with (a) x = 0.02, (b) x = 0.04, (c) x = 0.06, (d) x = 0.08 sintered at 900 °C for 6 h.

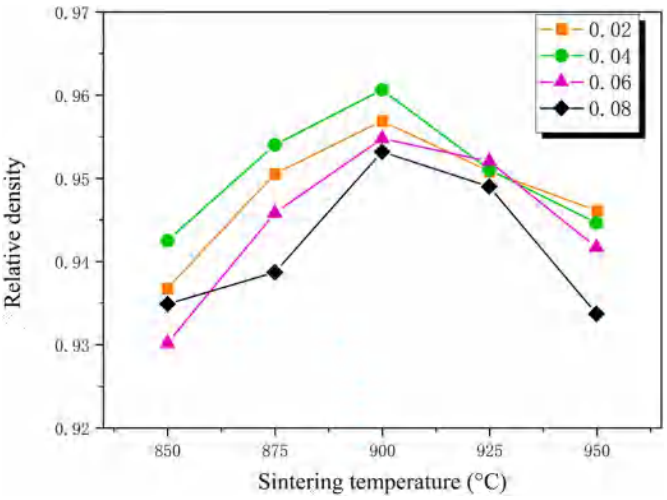

Fig. 3. The relative density of $Li_2Mg_3Ti_{1-x}(Al_{1/2}Nb_{1/2})_xO_6$-4wt%LiF ceramics *versus* sintered temperatures.

$_2Nb_{1/2})^{4+}$ composite ions, the relative density first goes up and then go down. When the substitution amount is 0.04 mol, achieves the maximum value of 96.2%. The experimental results indicate that the substitution of $(Al_{1/2}Nb_{1/2})^{4+}$ composite ions improves the densification of ceramics because the composite ions $(Al_{1/2}Nb_{1/2})^{4+}$ solid solution in ceramic crystals reduces the free energy, which promotes the sintering process. However, when $(Al_{1/2}Nb_{1/2})^{4+}$ substitution amount is too much, the relative density of ceramics decreases because the second phase is formed after LMTAN ceramics reach the solid solution limit. Moreover, it can be observed from Fig. 2 that the size of grain decreases and the size is not uniform, which reduces the density of ceramics, so the relative density decreases as well.

Fig. 4 displays the variations of the relative dielectric constant(ε_r) of LMTAN ceramics at different sintering temperatures. On the whole, the ε_r of LMTAN ceramics augments at first and then reduces with the increase of sintering temperature, which is in accordance with the changing trend of the density. On the other hand, when the sintering temperature is 900 °C and the composite ions substitution of $(Al_{1/2}Nb_{1/2})^{4+}$ is 0.02 mol, the ε_r reaches the best value, and the ε_r reduces then with the augment of the substitution, indicating that the substitution of $(Al_{1/2}Nb_{1/2})^{4+}$ ions reduces the ε_r value of $Li_2Mg_3TiO_6$-4wt%LiF ceramics. This phenomenon can be explained in two aspects. First of all, when $0.02 \leq x \leq 0.04$, $(Al_{1/2}Nb_{1/2})^{4+}$ and $Li_2Mg_3TiO_6$-4wt%LiF ceramic form a complete solid solution, ε_r mainly related to the size of the dielectric polarization rate, which can be get from the Shannon rule [31]. This rule is shown in eq (4), in which α means the polarization rate.

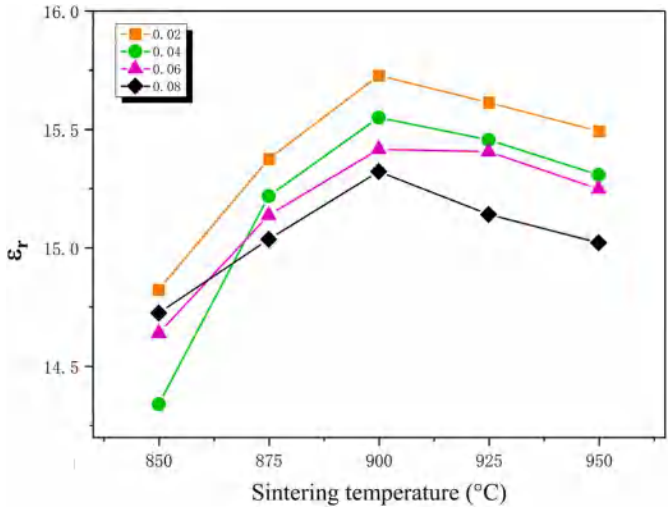

Fig. 4. The dielectric constant ε_r of $Li_2Mg_3Ti_{1-x}(Al_{1/2}Nb_{1/2})_xO_6$-4wt%LiF ceramics *versus* sintered temperatures.

$$\alpha(A_2BO_4) = 2\alpha(A^{2+}) + \alpha(B^{4+}) + 4\alpha(O^{2-}) \quad (4)$$

From this equation, for a given molecule formula, the polarizability can be summed by the rule that the total polarizability is equal to the sum of the polarizability of the decomposed parts.

According to Shannon rule, the dielectric polarization rate of $(Al_{1/2}Nb_{1/2})^{4+}$ (2.38 Å) is less than that of the Ti^{4+} ions (2.93 Å), so the dielectric constant of LMTAN ceramics will decrease if the $(Al_{1/2}Nb_{1/2})^{4+}$ replace the Ti^{4+} ions completely.

Secondly, when $x \geq 0.06$, the second phase $MgAl_2O_4$ ($\varepsilon_r = 8.8$) is generated, and the ε_r value continued to decrease according to the Lichtenecker rule, which is shown as follows.

$$\ln \varepsilon = \sum_i V_i \ln \varepsilon_i \quad (5)$$

where ε_i and V_i represent the relative permittivity and the volume fraction of the i-th phase, respectively.

For a particular material system, the product of Q and *f* would be a constant value. Therefore, $Q \times f$ value is often used to evaluate the quality factor of ceramics materials. Fig. 5 describes the $Q \times f$ value curves of LMTAN ceramics at different sintering temperatures. On the whole, the $Q \times f$ value improves at first and then declines with the increment of temperature, and reaches the maximum value at the optimal sintering temperature of 900 °C, which is consistent with the change of relative density. On the other hand, it can be observed that when the sintering temperature is 900 °C. With the increase of the $(Al_{1/2}Nb_{1/2})^{4+}$ substituted, the $Q \times f$ value also shows the similar trend that first increase and then decrease, reaching the maximum value of 154,000 Ghz when the substituted of $(Al_{1/2}Nb_{1/2})^{4+}$ content is 0.04 mol. The substitution of $(Al_{1/2}Nb_{1/2})^{4+}$ ions effectively improves the $Q \times f$ value of $Li_2Mg_3TiO_6$-4wt%LiF ceramics. Based on the previous analysis, the main reasons for the change of $Q \times f$ value are as follows: firstly, the introduction of $(Al_{1/2}Nb_{1/2})^{4+}$ ions reduces the surface free energy and promotes the densification process; second, when the substitution amount of $(Al_{1/2}Nb_{1/2})^{4+}$ ions is higher than 0.04 mol, the phase of

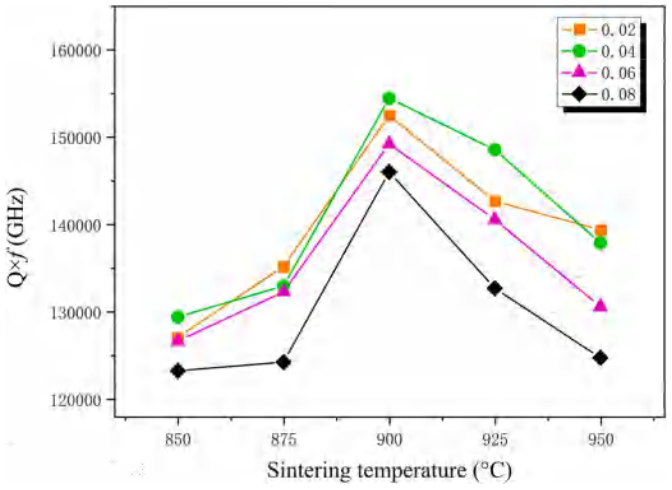

Fig. 5. The Q × *f* values of $Li_2Mg_3Ti_{1-x}(Al_{1/2}Nb_{1/2})_xO_6$-4wt%LiF ceramics *versus* sintered temperatures.

$MgAl_2O_4$ appears, which enhances the negative effect of crystal structure defects on LMTAN ceramics. Meanwhile, the Q × *f* value of $MgAl_2O_4$ is 68,900 GHz, far less than the Q × *f* value of $Li_2Mg_3TiO_6$-based ceramics. According to the Shannon rule, the Q × *f* value of LMTAN ceramics should decrease in this condition.

Finally, a comprehensive properties summary of LMTAN ceramics at the optimal sintering temperature has been summarized in Table 1. As is shown in this table, the resonant frequency temperature coefficient τ_f declined with the increase of $(Al_{1/2}Nb_{1/2})^{4+}$ content substituted. According to eq (6):

$$\tau_f = -\alpha_L - \frac{1}{2}\tau_\varepsilon \quad (6)$$

From this equation, the τ_f value is mainly related to α_L and τ_ε, where α_L is the linear expansion coefficient and τ_ε is relative dielectric constant temperature coefficient. The α_L of microwave medium is usually 10 ppm/°C, so τ_f is mainly decided by the relative dielectric constant temperature coefficient τ_ε. Generally, the bigger the dielectric constant is, the larger the positive value will appear in the temperature coefficient of resonance frequency. Meanwhile, ceramics with a small dielectric constant have a large negative resonance frequency temperature coefficient. When $0.02 \leq x \leq 0.04$, the τ_f value of LMTAN ceramics has a large negative value with the ϵ_r value decreases. The second phase $MgAl_2O_4$ generated when $x > 0.04$, according to the Lichtenecker rule, the τ_f value of $MgAl_2O_4$ is −78 ppm/°C, which is far less than the temperature coefficient of LMTAN ceramics, so τ_f has a more significant decline.

The microwave dielectric properties for different $Li_2Mg_3TiO_6$ based ceramics sintering at their optimum temperatures are shown in Table 2. For $Li_2Mg_3TiO_6$ ceramics, the best Q × *f* ~152,000 GHz and the relative stable τ_f ~-38.3 ppm/°C are obtained at 1350 °C, the sintering temperature is too high for its widely application. The addition of LiF as a common sintering aid to $Li_2Mg_3TiO_6$ ceramics can reduce the sintering temperature to 950 °C. But the properties especially the Q × *f* value decreases to 131,000 GHz compared with $Li_2Mg_3TiO_6$ ceramics, which can be attributed that the grain size deducts significantly while adding LiF promote sintering densification. Moreover, the $(Al_{1/2}Nb_{1/2})^{4+}$ ions are introduced into $Li_2Mg_3TiO_6$-4wt%LiF ceramics to replace Ti^{4+} to improve the Q × *f* value. Furthermore, $Li_2Mg_3Ti_{1-x}(Al_{1/2}Nb_{1/2})_xO_6$-4wt%LiF ceramics sintered at 900 °C for 6 h showed the best microwave dielectric properties of ε_r~15.54, Q × *f*~154,000 GHz and τ_f~-38.3 ppm/°C, which can be applied to LTCC application effectively.

Table 1
The relative density and dielectric properties of LMTAN ceramics at the optical sintering temperature.

$Li_2Mg_3Ti_{1-x}(Al_{1/2}Nb_{1/2})_xO_6$-4wt%LiF	R_d (%)	ϵ_r	Q × *f* (GHz)	τ_f(ppm/°C)
x = 0.02	95.6	15.72	152,000	−36.2
x = 0.04	96.2	15.54	154,000	−38.3
x = 0.06	95.5	15.41	149,000	−43.6
x = 0.08	95.3	15.32	146,000	−48.4

Table 2
The optimum sintering temperature and the most excellent microwave dielectric properties of $Li_2Mg_3TiO_6$ based ceramics.

Component	sintering temperature(°C)	ϵ_r	Q × *f* (GHz)	τ_f(ppm/°C)
$Li_2Mg_3TiO_6$	1350	15.2	152,000	−39 [10]
$Li_2Mg_3TiO_6$-4wt%LiF	950	16.2	131,000	−44 [19]
$Li_2Mg_3Ti_{1-x}(Al_{1/2}Nb_{1/2})_xO_6$-4wt%LiF	900	15.54	154,000	−38.3

4. Conclusions

In summary, this work presented the effects of the $(Al_{1/2}Nb_{1/2})^{4+}$ on the sintering characteristics and microwave dielectric properties of $Li_2Mg_3TiO_6$-4wt%LiF ceramics, which demonstrated that the compound ions doping could enhance the performance of the ceramics especially the Q × *f* value. The ceramics were synthesized by a conventional solid stated reaction method. Then we studied the phase composition, sintering characteristics and microwave dielectric properties of LMTAN ceramics. It could be concluded that the solid solubility limit of $(Al_{1/2}Nb_{1/2})^{4+}$ in the LMTAN is 0.04 mol, so the degree of lattice reaches the maximum when x is 0.04 as well. Moreover, at the optimal sintering temperature(900 °C), with the $(Al_{1/2}Nb_{1/2})^{4+}$ ions increased, the ε_r value decreased and the absolute value of τ_f augmented. Moreover, the Q × *f* value of ceramics was in accord with the relative density, which augmented at first until the doping content reached the solid solubility limit (0.04 mol) of the ceramics. Furthermore, the $Li_2Mg_3Ti_{0.96}(Al_{1/2}Nb_{1/2})_{0.04}O_6$-4wt%LiF ceramics sintered at 900 °C for 6 h showed the best microwave dielectric properties of ε_r~15.54, Q × *f*~154,000 GHz and τ_f~-38.3 ppm/°C.

Declaration of competing interest

Ping Zhang declares that she has no known competing financial interests or personal relationships that could have appeared to influence the work reported in this paper.

Gaowei Zhen declares that he has no known competing financial interests or personal relationships that could have appeared to influence the work reported in this paper.

Miaomiao Yang declares that she has no known competing financial interests or personal relationships that could have appeared to influence the work reported in this paper.

CRediT authorship contribution statement

Ping Zhang: Conceptualization, Methodology, Writing - review & editing, Validation. **Gaowei Zhen:** Data curation, Writing - original draft, Investigation, Software. **Miaomiao Yang:** Software, Investigation.

Acknowledgments

This work was supported by Major Projects of Science and Technology in Tianjin (No. 18ZXJMTG00020), and the National Natural Science Foundation of China (No. 61671323).

References

[1] K. Wakino, T. Nishikawa, Y. Ishikawa, H. Tamura, Dielectric resonator materials and their applications for mobile communication systems, Br. Ceram. Trans. J. 89 (1990) 39–43.

[2] J.-M. Le Floch, Y. Fan, G. Humbert, Q. Shan, D. Férachou, R. Bara-Maillet, M. Aubourg, J.G. Hartnett, V. Madrangeas, D. Cros, J.-M. Blondy, J. Krupka, M. E. Tobar, Invited Article, Dielectric material characterization techniques and designs of high-Q resonators for applications from micro to millimeter-waves frequencies applicable at room and cryogenic temperatures, Rev. Sci. Instrum. 85 (2014), https://doi.org/10.1063/1.4867461, 031301.

[3] I.M. Reaney, D. Iddles, Microwave dielectric ceramics for resonators and filters in mobile phone networks, J. Am. Ceram. Soc. 89 (2006) 2063–2072, https://doi.org/10.1111/j.1551-2916.2006.01025.x.

[4] W. Mao, Q. Yao, Y. Fan, Y. Wang, X. Wang, Y. Pu, X. Li, Combined experimental and theoretical investigation on modulation of multiferroic properties in $BiFeO_3$ ceramics induced by Dy and transition metals co-doping, J. Alloys Compd. 784 (2019) 117–124, https://doi.org/10.1016/j.jallcom.2018.12.381.

[5] Y. Zhou, R. Zhang, Y. Fan, Z. Wang, W. Mao, J. Zhang, Y. Min, J. Yang, Y. Pu, X. Li, Effect of Fe-site isovalent and aliovalent doping on the magnetic, electric and optical properties of $BiFe_{0.875}Cr_{0.125}O_3$, Solid State Commun. 270 (2018) 12–16, https://doi.org/10.1016/j.ssc.2017.11.004.

[6] R. Zhang, Y. Zhou, Y. Zhu, Y. Li, L. Chu, Y. Min, J. Zhang, J. Yang, X. Li, First principle investigations of the Pbnm phase $BiFeO_3$, $BiFe_{0.875}Mn_{0.125}O_3$ and $Bi_{0.875}X_{0.125}Fe_{0.875}Mn_{0.125}O_3$ (XBFM) (X = Ce, Gd, Lu), Mod. Phys. Lett. B 31 (2017) 1750304, https://doi.org/10.1142/S0217984917503043.

[7] W. Zhang, X. Zhu, L. Wang, X. Xu, Q. Yao, W. Mao, X. Li, Study on the magnetic and ferroelectric properties of $Bi_{0.95}Dy_{0.05}Fe_{0.95}M_{0.05}O_3$ (M = Mn, Co) ceramics, J. Supercond. Nov. Magnetism 30 (2017) 3001–3005, https://doi.org/10.1007/s10948-017-4267-2.

[8] R.J. Cava, Dielectric materials for applications in microwave communications, J. Mater. Chem. 11 (2001) 54–62, https://doi.org/10.1039/B003681L.

[9] W. Wersing, Microwave ceramics for resonators and filters, Curr. Opin. Solid State Mater. Sci. 1 (1996) 715–731, https://doi.org/10.1016/S1359-0286(96)80056-8.

[10] Z. Fu, P. Liu, J. Ma, X. Zhao, H. Zhang, Novel series of ultra-low loss microwave dielectric ceramics: $Li_2Mg_3BO_6$(B = Ti, Sn, Zr), J. Eur. Ceram. Soc. 36 (2016) 625–629, https://doi.org/10.1016/j.jeurceramsoc.2015.10.040.

[11] Z. Fu, J. Ma, X. Zhang, B. Wang, The effect of sintering agents on the sinter ability and dielectric properties of $Li_2Mg_3TiO_6$ ceramics, Ferroelectrics 510 (2017) 50–55, https://doi.org/10.1080/00150193.2017.1326803.

[12] J. Ma, Z. Fu, P. Liu, L. Zhao, B. Guo, Ultralow-fired $Li_2Mg_3TiO_6$-$Ca_{0.8}Sr_{0.2}TiO_3$ composite ceramics with temperature stable at microwave frequency, J. Alloys Compd. 709 (2017) 299–303, https://doi.org/10.1016/j.jallcom.2017.03.103.

[13] P. Zhang, H. Xie, Y. Zhao, M. Xiao, Microwave dielectric properties of low loss $Li_2(Mg_{0.95}A_{0.05})_3TiO_6$(A = Ca^{2+}, Ni^{2+}, Zn^{2+}, Mn^{2+}) ceramics system, J. Alloys Compd. 689 (2016) 246–249, https://doi.org/10.1016/j.jallcom.2016.07.198.

[14] P. Zhang, H. Xie, Y. Zhao, M. Xiao, Synthesis and microwave dielectric characteristics of high-Q $Li_2Mg_xTiO_{3+x}$ ceramics system, Mater. Res. Bull. 98 (2018) 160–165, https://doi.org/10.1016/j.materresbull.2017.10.012.

[15] T. Xie, L. Zhang, H. Ren, M. Dang, H. Wang, S. Jiang, X. Zhao, F. Meng, H. Lin, L. Luo, A novel temperature-stable and low-loss microwave dielectric using $Ca_{0.8}Sr_{0.2}TiO_3$- modified $Li_2Mg_3TiO_6$ ceramics, J. Mater. Sci. Mater. Electron. 28 (2017) 13705–13709, https://doi.org/10.1007/s10854-017-7214-x.

[16] H.L. Pan, L. Cheng, H.T. Wu, Relationships between crystal structure and microwave dielectric properties of $Li_2(Mg_{1-x}Co_x)_3TiO_6$ ($0 \le x \le 0.4$) ceramics, Ceram. Int. 43 (2017) 15018–15026, https://doi.org/10.1016/j.ceramint.2017.08.026.

[17] H.L. Pan, Y.W. Zhang, H.T. Wu, Crystal structure, infrared spectroscopy and microwave dielectric properties of ultralow-loss $Li_2Mg_3Ti_{0.95}(Mg_{1/3}Sb_{2/3})_{0.05}O_6$ ceramic, Ceram. Int. 44 (2018) 3464–3468, https://doi.org/10.1016/j.ceramint.2017.10.094.

[18] Y.K. Yang, H.L. Pan, H.T. Wu, Crystal structure, Raman spectra and microwave dielectric properties of $Li_2Mg_3Ti_{1-x}(Mg_{1/3}Nb_{2/3})_xO_6$ ($0 \le x \le 0.25$) ceramics, Ceram. Int. 44 (2018) 11350–11356, https://doi.org/10.1016/j.ceramint.2018.03.184.

[19] Z. Fu, P. Liu, J. Ma, X. Chen, H. Zhang, New high Q low-fired $Li_2Mg_3TiO_6$ microwave dielectric ceramics with rock salt structure, Mater. Lett. 164 (2016) 436–439, https://doi.org/10.1016/j.matlet.2015.11.046.

[20] Y.-Z. Hao, H. Yang, G.-H. Chen, Q.-L. Zhang, Microwave dielectric properties of Li_2TiO_3 ceramics doped with LiF for LTCC applications, J. Alloys Compd. 552 (2013) 173–179, https://doi.org/10.1016/j.jallcom.2012.10.110.

[21] Z. Xiong, B. Tang, Z. Fang, C. Yang, S. Zhang, Crystal structure, Raman spectroscopy and microwave dielectric properties of $Ba_{3.75}Nd_{9.5}Ti_{18-z}(Al_{1/2}Nb_{1/2})_zO_{54}$ ceramics, J. Alloys Compd. 723 (2017) 580–588, https://doi.org/10.1016/j.jallcom.2017.06.258.

[22] G.H. Chen, J.S. Chen, X.L. Kang, Y. Luo, Q. Feng, C.L. Yuan, Y. Yang, T. Yang, Structural and microwave dielectric properties of new $CaTi_{1-x}(Al_{0.5}Nb_{0.5})_xO_3$ thermally stable ceramics, J. Alloys Compd. 675 (2016) 301–305, https://doi.org/10.1016/j.jallcom.2016.03.059.

[23] T. Zhang, R. Zuo, J. Zhang, Structure, microwave dielectric properties, and low-temperature sintering of acceptor/donor codoped $Li_2Ti_{1-x}(Al_{0.5}Nb_{0.5})_xO_3$ ceramics, J. Am. Ceram. Soc. 99 (2016) 825–832, https://doi.org/10.1111/jace.14055.

[24] H. Chen, Phase evolution and microwave dielectric properties of $Ca_{0.61}Nd_{0.26}Ti_{1-x}(Al_{1/2}Nb_{1/2})_xO_3$ ceramics ($0 \le x \le 0.2$), Ceramics (2016) 1–5, https://doi.org/10.13168/cs.2016.0052.

[25] G. Chen, H. Xu, C. Yuan, Microstructure and microwave dielectric properties of $Li_2Ti_{1-x}(Zn_{1/3}Nb_{2/3})_xO_3$ ceramics, Ceram. Int. 39 (2013) 4887–4892, https://doi.org/10.1016/j.ceramint.2012.11.081.

[26] X. Guo, B. Tang, J. Liu, H. Chen, S. Zhang, Microwave dielectric properties and microstructure of $Ba_{6-3x}Nd_{8+2x}Ti_{18-y}(Cr_{1/2}Nb_{1/2})_yO_{54}$ ceramics, J. Alloys Compd. 646 (2015) 512–516, https://doi.org/10.1016/j.jallcom.2015.05.202.

[27] P. Zhang, L. Liu, M. Xiao, Y. Zhao, A novel temperature stable and high Q microwave dielectric ceramic in $Li_3(Mg_{1-x}Mn_x)_2NbO_6$ system, J. Mater. Sci. Mater. Electron. 28 (2017) 12220–12225, https://doi.org/10.1007/s10854-017-7037-9.

[28] L. Li, H. Sun, X. Lv, S. Li, A new microwave dielectric material $ZnZrNbTaO_8$, Mater. Lett. 160 (2015) 363–365, https://doi.org/10.1016/j.matlet.2015.08.020.

[29] K.X. Hu, D. Zhang, B. Su, T.W. Button, I.P. Jones, Influence of manganese segregation on the grain size in (Ba,Sr)TiO_3-based ceramics, Microsc. Microanal. 11 (2005) 1728–1729, https://doi.org/10.1017/S1431927605505142.

[30] E. Li, X. Yang, H. Yang, H. Yang, H. Sun, Y. Yuan, S. Zhang, Crystal structure, microwave dielectric properties and low temperature sintering of $(Al_{0.5}Nb_{0.5})^{4+}$ co-substitution for Ti^{4+} of $LiNb_{0.6}Ti_{0.5}O_3$ ceramics, Ceram. Int. 45 (2019) 5418–5424, https://doi.org/10.1016/j.ceramint.2018.11.243.

[31] R.D. Shannon, Dielectric polarizabilities of ions in oxides and fluorides, J. Appl. Phys. 73 (1993) 348–366, https://doi.org/10.1063/1.353856.